Phase Diagram, Stability, and Overcharging of Lamellar Cationic Lipid–DNA Self-Assembled Complexes

I. Koltover, T. Salditt, and C. R. Safinya
Materials Department, Physics Department and Biochemistry and Molecular Biology Program, University of California, Santa Barbara, California 93106

ABSTRACT Cationic lipid–DNA (CL-DNA) complexes comprise a promising new class of synthetic nonviral gene delivery systems. When positively charged, they attach to the anionic cell surface and transfer DNA into the cell cytoplasm. We report a comprehensive x-ray diffraction study of the lamellar CL-DNA self-assemblies as a function of lipid composition and lipid/DNA ratio, aimed at elucidating the interactions determining their structure, charge, and thermodynamic stability. The driving force for the formation of charge-neutral complexes is the release of DNA and lipid counterions. Negatively charged complexes have a higher DNA packing density than isoelectric complexes, whereas positively charged ones have a lower packing density. This indicates that the overcharging of the complex away from its isoelectric point is caused by changes of the bulk structure with absorption of excess DNA or cationic lipid. The degree of overcharging is dependent on the membrane charge density, which is controlled by the ratio of neutral to cationic lipid in the bilayers. Importantly, overcharged complexes are observed to move toward their isoelectric charge-neutral point at higher concentration of salt co-ions, with positively overcharged complexes expelling cationic lipid and negatively overcharged complexes expelling DNA. Our observations should apply universally to the formation and structure of self-assemblies between oppositely charged macromolecules.

INTRODUCTION

Cationic lipid–DNA (CL-DNA) complexes are compact, ordered macromolecular self-assemblies that have recently received much attention because of their potential use as nonviral gene carriers (Felgner, 1997; Felgner and Rhodes, 1991). It has been established that positively charged CL-DNA complexes can deliver DNA into cultured cells by binding electrostatically to their anionic membranes. Although the transfection efficiencies of CL-DNA vectors are lower than typically achieved with virus-based gene delivery techniques, they offer several critical advantages: nonimmunogenicity, low toxicity, and ease of large-scale production. Most importantly, DNA of any large length can potentially be delivered with the CL-DNA complexes, and recent experiments used this technique to transfer ~1 Mbp sections of the human artificial chromosomes (HAC) (Harrington et al., 1997). Preliminary experiments have demonstrated the promise of CL-DNA complexes as vectors for in-vivo use in targeted organs (Nabel et al., 1993; Zhu et al., 1993).

The complexes are often prepared using mixtures of cationic and neutral (helper) lipids. Transfection rates have been shown to vary as a function of lipid composition and lipid/DNA ratio, but until recently the findings were empirical, partly because little was known about the complex structure and interaction with cell membranes. It has been shown previously that CL-DNA complexes have ordered liquid-crystalline structure (Rädler et al., 1997; Gustafsson et al., 1995; Lasic et al., 1997). Its topology is controlled by the choice of the helper lipid type: lamellar (L_α^c, Fig. 1) complexes, with DNA intercalated between planar lipid membranes, can be converted into inverted hexagonal (H_{II}^c) complexes with DNA confined in inverted lipid micelles either by changing the membrane spontaneous curvature or the membrane flexibility (Koltover et al., 1998). However, within a given type of complex structure, there remains a question about the quantitative nature of interactions driving the complex self assembly and determining its charge, colloidal behavior and stability against dissociation.

More generally, the CL-DNA complex is an example of self-assembled structures formed nonspecifically between DNA and molecules of opposite charge. These abound in biology and include complexes of DNA with histones, DNA-binding proteins, and cationic ligands (drugs). Simple Coulomb attraction cannot explain the formation, compactness, and stability of these self-assemblies, because highly charged macromolecules in solution are always surrounded by a sheath of oppositely charged counterions. For planar lipid bilayers or long cylindrically-shaped macromolecules such as DNA, nonlinear Poisson–Boltzmann theory predicts that most of the counterions are confined to the immediate vicinity of their surface, the phenomenon known as counterion condensation (Manning, 1969; Le Bret and Zimm, 1984). When the compact DNA-polycation self-assemblies are formed, opposite charges of the macromolecules neutralize each other and release their counterions into solution. The resulting entropy gain ($\sim k_B T$ per released counterion) is large when binding macromolecules have many charged groups and has been shown to be the dominant interaction in formation of many DNA–macroion complexes (Mascotti and Lohman, 1990; Misra et al., 1994; Schlax et al., 1995).

Received for publication 26 October 1998 and in final form 30 April 1999.
Address reprint requests to Dr. Cyrus Safinya, Materials Department, University of California, MRL Bldg., Room 2208, Santa Barbara, CA 93106. Tel.: 805-893-8635; Fax: 805-893-7221; E-mail: safinya@engineering.ucsb.edu.

0006-3495/99/08/915/10 $2.00

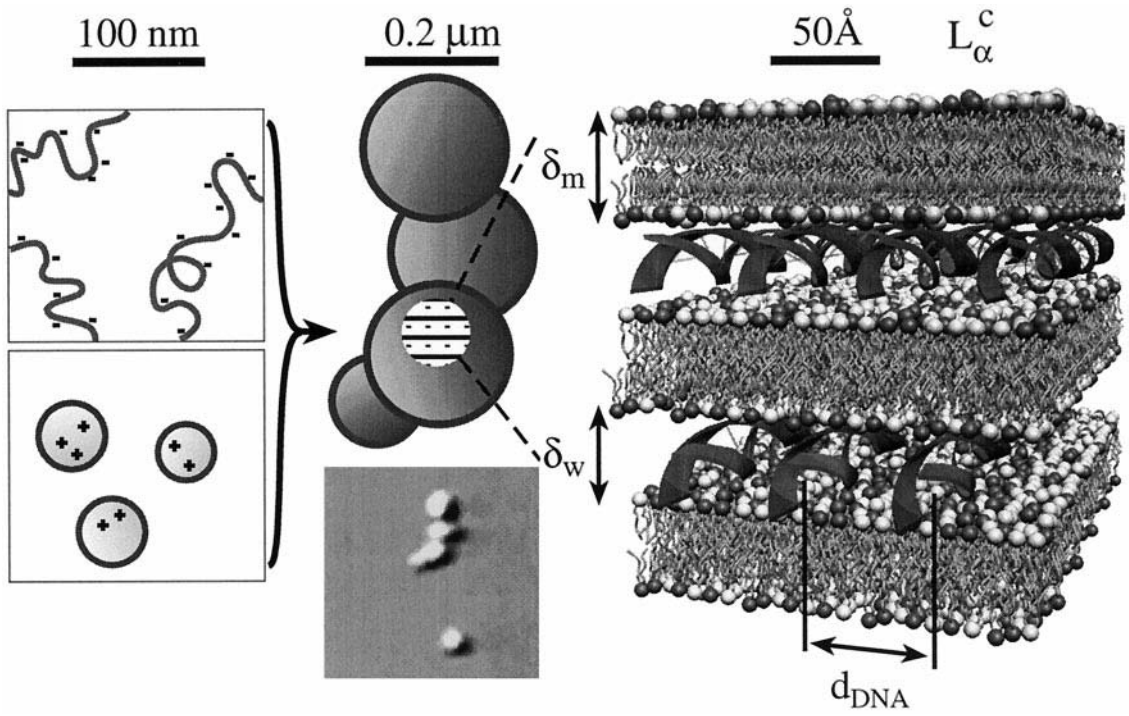

FIGURE 1 Linear DNA molecules are condensed in the mixture with unilamellar cationic liposomes (*left*), whereby both lipid and DNA undergo a complete topological transformation into compact quasispherical complex particles. Complexes of low net charge form string-like colloidal aggregates, easily visualized with DIC microscopy (*center*). Internally, the complexes have ordered lamellar L_α^c structure (*right*).

The counterion release mechanism, as described above, predicts the formation of only charge-neutral complexes, because it implies one-to-one binding of opposite macroion charges. However, the functionality of many DNA self-assemblies critically depends on their non-zero charge. CL-DNA complexes must be cationic to bind to cell surfaces. Moreover, histone-DNA nucleosomes in-vitro are negatively charged at low ionic strength and exhibit a reversible condensation transition to chromatin fibers in the presence of positively charged linker histones H_1 and elevated salt concentrations (~100 mM) (Ramakrishnan, 1997). Much remains unknown about the stability of polyelectrolyte self-assemblies in salt solutions, which influences the CL-DNA complex behavior inside a cytoplasm, where the ionic strength can vary greatly. Thus, a quantitative study of the interactions driving DNA–macroion complex formation and stability is highly desirable.

The lamellar L_α^c CL-DNA complexes have a highly ordered structure (Fig. 1), which enables us to use x-ray diffraction to quantify the DNA packing density and to relate the macroscopic properties and the internal microscopic structure of the complexes. We maintain the L_α^c complex topology by using the mixture of cationic and neutral (helper) lipids favoring planar lipid bilayers. Within this constraint, we examine the complex overcharging as a function of lipid membrane charge density and show that it is accompanied by the changes in the DNA packing inside the complex. We investigate the possibility that these are caused by the osmotic pressure of counterions, which pushes excess lipid or DNA into the counterion-free isoelectric complex (Bruinsma, 1998; Harries et al., 1998). We relate this finding to the observed changes in the CL-DNA complex structure and stability as a function of ionic strength and also demonstrate the presence of hydration repulsion between the DNA strands inside the complex.

METHODS AND MATERIALS

Lamellar CL-DNA complexes were formed by mixing small unilamellar liposomes (~50 nm), prepared by sonicating the mixtures of cationic lipid dioleoyl trimethylammonium propane (DOTAP) (MW(DOTAP) = 698.6) and neutral lipid dioleoyl phosphatidylcholin (DOPC) (MW(DOPC) = 705, Avanti Polar Lipids, Alabaster, AL), with linear λ-DNA (48,502 bp, average MW(bp) = 649, New England Biolabs, Beverly, MA) purified by ethanol precipitation (Fig. 1, *left*). Lipid mixture composition can be changed by varying the weight fraction of DOPC Φ_{PC} = (weight of DOPC)/(total lipid weight = L). Because the molecular weights of DOPC and DOTAP are similar, Φ_{PC} is also the mole fraction of neutral lipid in the bilayer and $\Phi_{TAP} = 1 - \Phi_{PC}$ is the mole fraction of cationic lipid DOTAP. Each DOTAP molecule has one positive charge/head group of area $a \approx 70$ Å^2, whereas the DNA carries two negative charges/bp ($2e^-$/3.4 Å). The CL-DNA mixture is stoichiometrically charge neutral when the numbers of DOTAP molecules and DNA bases are equal, or when ρ = (weight DOTAP)/(weight DNA = D) = $\rho^{iso} = 2 \times$ MW(DOTAP)/MW(bp) ≈ 2.2. Varying ρ changes the overall charge of the DNA-lipid system. Thus, Φ_{PC} and ρ comprise two independent axis of the CL-DNA complex composition phase diagram.

During the complex formation, both lipid and DNA undergo a complete topological transformation into compact, ordered particles of ~0.2 μm diameter (Fig. 1, *center top*). The complexes are easily visualized in an optical microscope as dynamic aggregates of individual ~0.2 μm particles

which aggregate into larger assemblies when the complexes are charge-neutral (Fig. 1, *center bottom*). The high optical contrast of the complexes stems from their ordered lamellar internal structure (Fig. 1, *left*), which makes them birefringent. The complex consists of alternating layers of lipid and DNA (Fig. 1, *right*) with periodicity $d = \delta_m + \delta_w$, where δ_m is the thickness of lipid bilayer and $\delta_w = 25$ Å is the thickness of the DNA monolayer (with a bound water layer). In DOPC/DOTAP complexes, δ_m increases from 35 to 44 Å, increasing with Φ_{PC}, because DOPC molecule is longer than DOTAP and because the headgroup area (and therefore bilayer thickness) of the lipids may vary slightly to accommodate the projected area/anionic group (approximately $2e^-$/68 Å) of the DNA molecule. To form a compact spherical object, lamellar DNA-lipid stacks have to curve near the complex wall, forming liquid-crystalline defects characteristic of smectic phases (Rädler et al., 1997). Significantly, DNA monolayers in the L_α^c complexes are ordered in a one-dimensional lattice with well-defined spacing d_{DNA} between the DNA rods forming a two-dimensional smectic liquid crystal (Salditt et al., 1997).

The structure shown in Fig. 1 has been derived from the high-resolution x-ray diffraction measurements of dense complex suspensions (95% water). Typical powder SAXS scans of one-phase lamellar complexes (bottom three scans of Fig. 2 *a*) exhibit a set of sharp, periodically spaced reflections at $q_{00l} = 2\pi l/d$ and a broad peak at $q_{DNA} = 2\pi/d_{DNA}$. The former are due to the lamellar bilayer-DNA structure with period d and the latter to the smectic structure of DNA arrays with spacing d_{DNA}. The DNA peak is broader than the lamellar ones because the two-dimensional smectic liquid crystal is less stable against thermal disorder than the three-dimensional smectic of the bilayer-DNA (Salditt et al., 1997). High-resolution synchrotron small-angle x-ray diffraction (SAXS) measurements were done at Stanford Synchrotron Radiation laboratory, while the lower-resolution data were collected in-house using a small-angle diffraction apparatus with an image-plate area detector (MAR Research, Hamburg, Germany).

The size and the ζ-potential (electrostatic potential near the surface) of the complexes were measured in more dilute samples, having concentrations equal to those usually used for transfection of cells (1/100 of x-ray samples) (Brookhaven Instruments particle size analyzer and zeta-meter, Holtsville, NY). We have shown previously that the complex structure is independent of the overall sample concentration (Rädler et al., 1997; Koltover et al., 1998). To check for the phase separation of excess DNA or lipid from the complex, we fluorescently labeled lipid with DHPE-Texas Red and DNA with YoYo-1 iodide (Molecular Probes, Eugene, OR). Complexes were observed using an inverted microscope with a 60× oil-immersion objective. The ionic strength in our samples was controlled by adding known amounts of NaCl to the solution. The resulting CL-DNA structures were independent of the order in which the three components of the samples (DNA, liposomes, monovalent salt) were mixed.

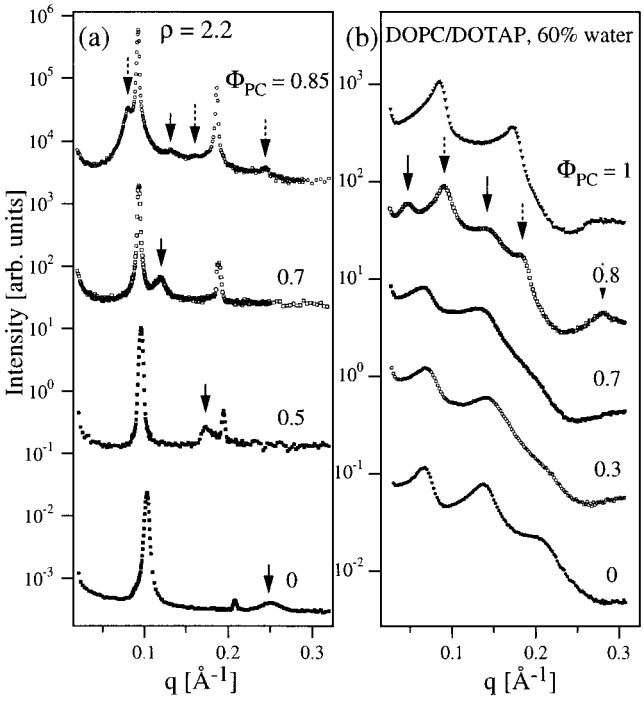

FIGURE 2 (*a*) Synchrotron SAXS scans of isoelectric CL-DNA complexes as a function of increasing Φ_{PC} (decreasing membrane charge density). (*b*) In-house SAXS scans of DOPC/DOTAP mixtures with 60% water and no added DNA. Pure DOPC (*top scan*) can be diluted only to ~43% water. Therefore, DOPC/DOTAP membranes can take in more water only when the lipids remain mixed (i.e., forming sufficiently charged membranes due to the presence of DOTAP). This is the case for the bottom three scans at $\Phi_{PC} = 0$, 0.3, and 0.7. The scan at $\Phi_{PC} = 0.8$ exhibits two sets of lamellar peaks, indicating lipid demixing into DOTAP-rich (*solid arrows*) and DOPC-rich (*dashed arrows*) phases.

RESULTS

We begin by investigating the behavior of complexes at low ionic strength (no added salt) along the Φ_{PC} axis in the phase diagram. Fig. 2 *a* shows a set of SAXS scans of complexes with fixed $\rho = \rho^{iso} = 2.2$ (isoelectric point) and increasing Φ_{PC}. For $\Phi_{PC} \leq 0.75$ the x-ray data show that the complexes remain lamellar and the DNA peak (*solid arrows*) shifts to smaller q with increasing Φ_{PC}. This means that DNA strands move apart as a function of decreasing membrane charge density $\sigma_c = (1 - \Phi_{PC})/a$. Microscopic observations confirm that, in this regime, the complexes remain one-phase, with no excess DNA or liposomes.

If all lipid and DNA counterions are released during the formation of an isoelectric CL-DNA complex, then, within the complex volume, the total number of cationic lipid headgroups should be equal to the number of anionic phosphates on the DNA backbone. Therefore, the average charge densities of membrane and DNA are matched, meaning that inside the complex the DNA chains occupy all of the available area S_m of cationic lipid membranes. The average spacing d_{DNA} between the DNA molecules in an isoelectric complex can then be simply expressed in terms of the average anionic charge/length of DNA λ and cationic charge/area of lipid Σ_c within the CL-DNA complex (Fig. 3 *b*),

$$d_{DNA} = \lambda/\Sigma_c. \quad (1)$$

Furthermore, because all lipid and DNA in stoichiometrically charge-neutral ($\rho = \rho^{iso} = 2.2$) mixtures associate within the isoelectric complexes (with no excess material), the DNA and membrane areas can be derived from their volume fractions and weights in the complex. The volume fraction of DNA chains confined between the membranes in the complex structure of Fig. 1 is $\Phi_{DNA} = v_D/(v_w + v_D)$, where v_D and v_w are volumes of DNA and water in the complex. Because the DNA and lipid areas are matched, $v_w + v_D = \delta_w S_m$ and $S_m = v_m/\delta_m$, where v_m is the membrane volume. Therefore, $v_w = v_m(\delta_w/\delta_m) - v_D$ and

$$\Phi_{DNA} = \frac{\delta_m}{\delta_w}\frac{v_D}{v_m} = \frac{\delta_m}{\delta_w}\frac{\rho_L D}{\rho_D L}, \quad (2)$$

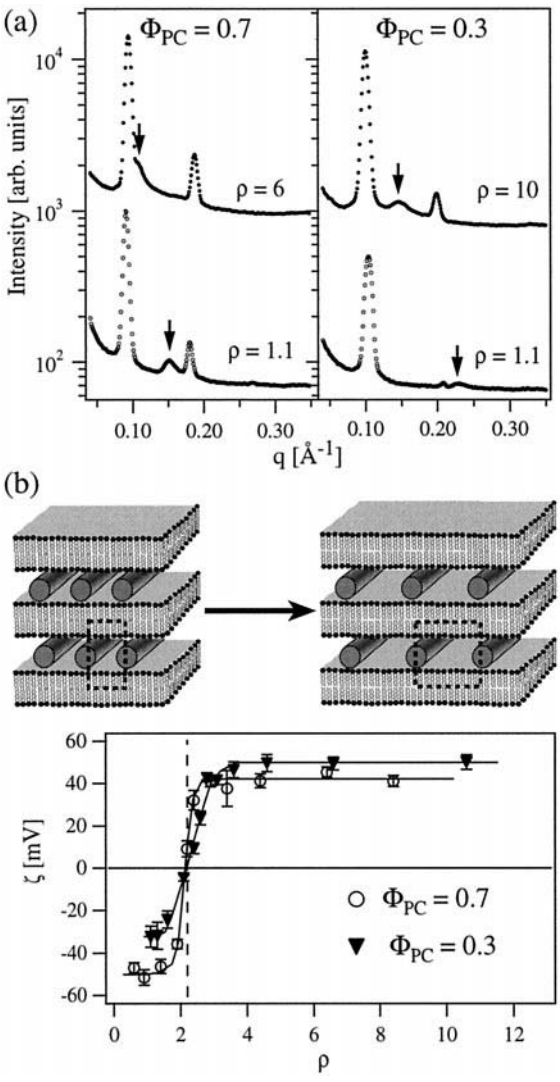

FIGURE 3 (*a*) In-house SAXS scans of complexes with two fixed Φ_{PC} and varying cationic/anionic charge ratio ρ. (*b*) Variation of the complex ζ-potential with changing ρ. The vertical line marks the isoelectric point ($\rho = 2.2$). Solid lines through the data are guides to the eye only. Also shown is a schematic of the corresponding real-space complex structure variation, where the dashed rectangles indicate the complex unit cell of height δ_w and width d_{DNA}.

where $\rho_D = 1.7$ g/cm^3, $\rho_L = 1.07$ g/cm^3 are densities of DNA and lipid, respectively, and L, D are total weights of lipid and DNA in the mixture. Assuming an equidistant (smectic) arrangement of DNA chains, we can also write

$$\Phi_{DNA} = \frac{N(\lambda)A_D L(\lambda)}{N(\lambda)d_{DNA}\delta_w L(\lambda)} = \frac{A_D}{d_{DNA}\delta_w}. \quad (3)$$

Here, $A_D \approx 190$ Å^2 is the cross-section area of DNA molecule, $N(\lambda)$ is the number of DNA chains in the complex, and $L(\lambda)$ = contour length of λ-DNA = 48502 × 3.4 Å $\{A_D = Wt(\lambda)/[\rho_D L(\lambda)]$ with $Wt(\lambda)$ = weight of λ-DNA = $32 \times 10^6/(6.022 \times 10^{23})g\}$.

Comparing the two expressions Eqs. 2 and 3 for Φ_{DNA}, we obtain the equation for the spacing between the DNA chains in isoelectric complexes,

$$d_{DNA} = d_{DNA}^{iso} = (A_D\rho_D/D)/(\delta_m\rho_L/L) = (A_D\rho_D/\delta_m\rho_L) \times \rho^{iso}/(1 - \Phi_{PC}). \quad (4)$$

This expression relies on the assumption of the complete counterion release from the isoelectric complexes, smectic DNA arrangement (independently confirmed from the width and shape of the DNA correlation peak (Salditt et al., 1997) and the experimentally observed complete association of all lipid and DNA within the charge-neutral complexes. Using Eq. 4 with the measured $\delta_m = d - \delta_w$ we obtain $d_{DNA} = 19.3$, 34.8, 52.7 Å for samples with $\Phi_{PC} = 0$, 0.5, 0.7 shown in Fig. 2. Comparing this with the measured values $d_{DNA} = 25.1$, 35.4, 52.9 Å, we see that the complete counterion release mechanism based Eq. 1 predicts well the structure of charge-neutral complexes when the calculated d_{DNA} is larger then the diameter of a hydrated DNA molecule (24 Å) (see also [Rädler et al., 1997] and the summary of the $d_{DNA}(\Phi_{PC})$ data in Fig. 4 *c*). Therefore, there are almost no counterions inside the one-phase isoelectric CL-DNA complexes for all but the smallest Φ_{PC}. For the smallest $\Phi_{PC} = 0$ the predicted d_{DNA} is smaller then the observed value due to the molecular crowding within the complex.

Note, that the membrane thickness increases with the Φ_{PC}, as described above: $\delta_m = 34.5$, 38.2 and 42.0 Å for $\Phi_{PC} = 0$, 0.5, 0.7, resulting in a deviation from a simple linear increase of d_{DNA} with $1/(1 - \Phi_{PC})$. This also means that the effective cationic charge per unit cell Σ_c in Eq. 1 is different from the simple geometric value $\sigma_c = (1 - \Phi_{PC})/a$. Hence, a careful calculation with matching of the DNA and lipid volumes (such as Eqs. 2 and 3) is required to correctly predict d_{DNA}. The nearly complete neutralization of the CL-DNA complex (i.e., complete counterion release) exactly at $\rho = 2.2$ is possible because the projected charge density of DNA (two anionic charges per 68 Å^2) is closely matched by two cationic head groups on DOTAP with area $a \approx 70$ Å^2 each. A recent direct solution conductivity measurement of the number of counterions released during the complex formation confirms this result (Rädler, personal communication).

SAXS measurements indicate that the DNA lattice cannot be diluted beyond $\Phi_{PC} = 0.75$. This is demonstrated by the scan at $\Phi_{PC} = 0.85$ in Fig. 2 *a*, where the lamellar complex peaks ($q_{001} = 0.093$ Å^{-1}) are still sharp, but the DNA peak at $q_{DNA} = 0.13$ Å^{-1} has shifted to larger q than at $\Phi_{PC} = 0.75$ ($q_{001} = 0.09$ Å^{-1}, $q_{DNA} = 0.11$ Å^{-1}). The additional peaks at $q = 0.082$, 0.164, and 0.246 Å^{-1} (*broken arrows*) are consistent with a membrane stack of periodicity $d_b = 76.5$ Å, equal to the periodicity of pure DOPC bilayers in excess water. Therefore, for $\Phi_{PC} > 0.75$, excess neutral DOPC lipid demixes from the DOPC/DOTAP membranes instead of remaining within the CL-DNA complex and further separating the DNA strands. Using Eq. 4 with the measured q_{DNA} at $\Phi_{PC} = 0.85$, we find that only 65% DOPC remains in the complex, which is also consistent with

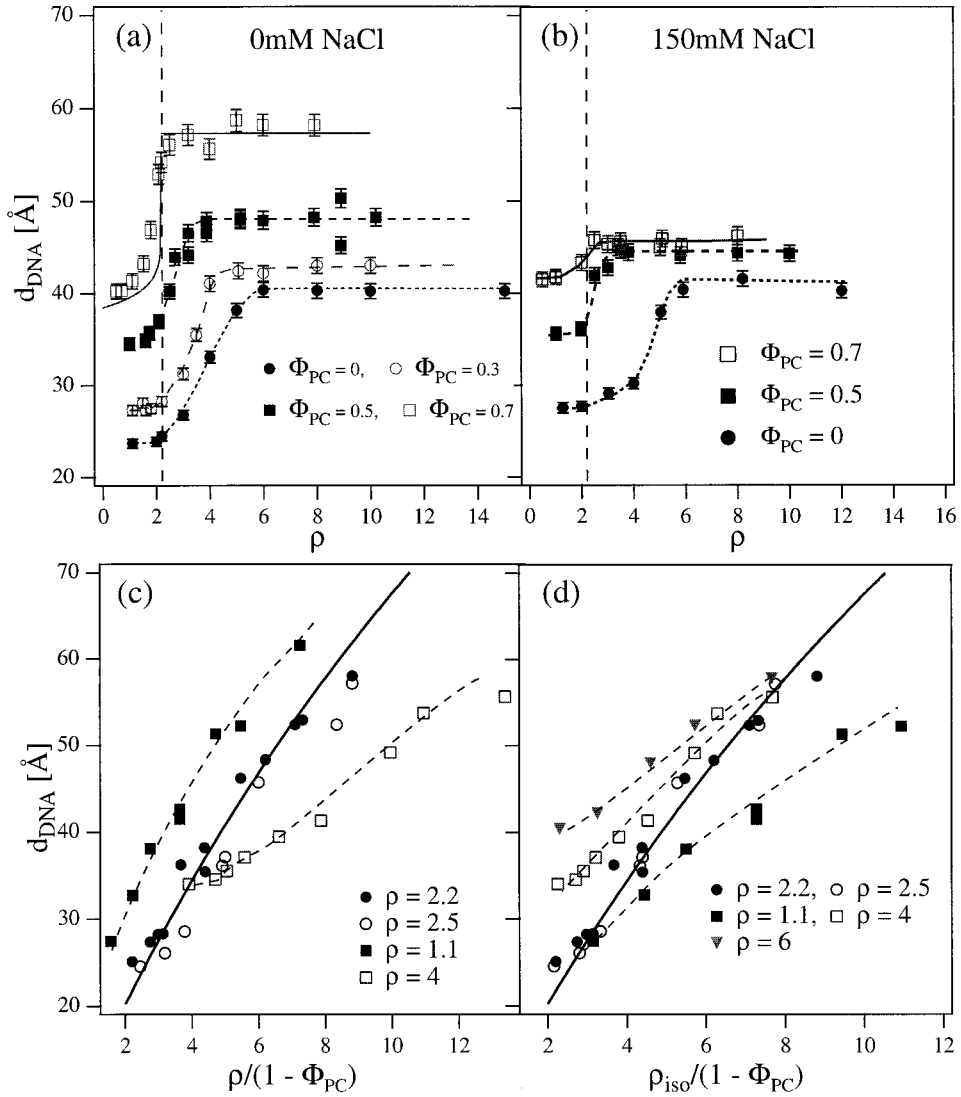

FIGURE 4 (*a*) Variation of DNA packing with ρ in complexes with fixed Φ_{PC} and no salt. Vertical dashed line indicates isoelectric point. The solid line through the data at $\Phi_{PC} = 0.7$ is the result of nonlinear Poisson–Boltzman theory for complexes with low membrane charge density (Bruinsma, 1998). The dashed lines are guides to the eye. The complexes are one-phase in the region of increasing d_{DNA}, coexisting with DNA at lower ρ and with lipid at higher ρ. (*b*) Same as (*a*) at 150 mM NaCl. All lines are guides to the eye. (*c*) Variation of d_{DNA} with changing Φ_{PC} in complexes with different fixed ρ. Solid line is the prediction of Eq. 4 for isoelectric complexes, while dashed lines are guides to the eye. (*d*) Same as (*c*) with the data scaled to $\rho_{iso} = 2.2$.

the shifted position of lamellar peak. We have found that DOPC/DOTAP mixtures without DNA also demix at $\Phi_{PC} \sim 0.75$, while forming stable one-phase lipid bilayer stacks at lower DOPC content (Fig. 2 *b*). Therefore, the upper limit of CL-DNA complex stability at $\Phi_{PC} = 0.75$ is set by the lipid demixing in the DOPC/DOTAP bilayers independent of the charge ratio ρ of DNA and lipid. The lipids remain mixed at low Φ_{PC} because electrostatic repulsion favors dispersion of DOTAP in lipid bilayers.

The behavior of CL-DNA complexes as a function of DOTAP/DNA charge ratio ρ is illustrated in Fig. 3. The system remains one-phase complex only close to the isoelectric point ($\rho = \rho^{iso} = 2.2$), and separates into complex + excess liposomes for $\rho > 2.2$ and complex + excess DNA for $\rho < 2.2$. Measurements of the complex ζ-potential (Fig. 3 *b*) show charge reversal at $\rho = 2.2$ for all Φ_{PC}, from negative at $\rho < 2.2$ to positive at $\rho > 2.2$. The complex structure also changes as a function of ρ, with smaller d_{DNA} for $\rho < 2.2$ and larger for $\rho > 2.2$ (Fig. 3 *b*), but remains constant away from the isoelectric point, with fixed d and d_{DNA}. This can be seen in the SAXS scans of Fig. 3 *a*, where d_{DNA} changes with ρ from 27.3 Å to 43 Å at constant $\Phi_{PC} = 0.3$ and from 41.3 Å to 58.2 Å at $\Phi_{PC} = 0.7$. Comparing this to $d^{iso}_{DNA} = 28.3$ Å ($\Phi_{PC} = 0.3$) and $d^{iso}_{DNA} = 52.9$ Å ($\Phi_{PC} = 0.7$) measured in the isoelectric complexes, we find that the positively charged complexes adsorb excess lipid into their bulk, while the negatively charged ones have surplus bulk DNA. This seemingly contradicts the counterion release prediction of neutral complex with all of the excess lipid and DNA expelled into solution. Note, that lamellar repeat distance d does not change significantly as a function of ρ, so that DNA remains tightly bound to lipid bilayers.

We show in Fig. 4 *a* a set of $d_{DNA}(\rho)$ curves for complexes with four different Φ_{PC}, which constitute adsorption isotherms of DNA and lipid into the complexes of fixed bilayer charge densities. For all investigated Φ_{PC}, d_{DNA} deviates significantly from d^{iso}_{DNA} in charge-neutral complexes. In fact, the complex seems to avoid the structure expected from a simple counterion-release mechanism. We have observed coexistence between complexes and excess

DNA or liposomes in the regions with constant d_{DNA}, whereas the complexes remain single phase when d_{DNA} increases with ρ close to the isoelectric point. The slope of the $d_{DNA}(\rho)$ increase is inversely proportional to $1/(1 - \Phi_{PC})$ (Fig. 4 *a*), consistent with Eq. 1, which always holds for one-phase complexes. The curves at different Φ_{PC} are distinct, shifting to lower ρ with the decreasing bilayer charge density σ_c. Because the charge reversal occurs at $\rho = 2.2$ independent of Φ_{PC}, this implies that the complexes with lower Φ_{PC} continue absorbing excess cationic lipid and remain one-phase for higher ρ than the ones with higher Φ_{PC}. This is consistent with the observation that $\zeta(\Phi_{PC} = 0.3) > \zeta(\Phi_{PC} = 0.7)$ in cationic complexes (Fig. 3 *b*). In contrast, complexes with lower Φ_{PC} take in more DNA starting at smaller ρ, resulting in the overall shift of $d_{DNA}(\rho)$ curves of Fig. 4 *a* and $\zeta(\Phi_{PC} = 0.3) > \zeta(\Phi_{PC} = 0.7)$ in anionic complexes. The reversal of the complex ζ-potential exactly at $\rho = 2.2$ shows that it is determined by the overall bulk DOTAP/DNA ratio, which is also underscored by the simultaneous variation of complex charge and DNA packing density.

To understand the interactions determining CL-DNA complex charge and structure (d_{DNA}) when $\rho \neq 2.2$, we must consider the whole system of complex + excess cationic lipid bilayer or complex + excess anionic DNA, together with their respective counterions (Bruinsma, 1998). Both free (not complexed) DNA and free bilayer have large free energies in low ionic strength solution, because they are charged and have a low-entropy layer of counterions confined either 1-dimensionally to DNA or 2-dimensionally near membrane surfaces. At the same time, there exists a counterion vacuum inside a $\rho = \rho^{iso} = 2.2$ charge-neutral complex, because all the lipid and DNA counterions were released during its formation. An additional DNA molecule can lower its free energy by entering the complex and releasing bound Na^+ counterions into the large 3-dimensional internal volume of the complex (Fig. 5). Thus, excess DNA can be driven into the isoelectric complex by an osmotic pressure of its confined counterions leading to the reduction of d_{DNA} and negative overcharging. The DNA intake will not continue indefinitely, due to the increase of counterion concentration inside the complex and, more importantly, because of electrostatic repulsion of additional DNA molecules, whose anionic charge is not compensated by the cationic charge of bound lipids.

Conversely, an analogous mechanism can lead to the intake of excess bilayer lipids. Because there are no counterions inside an isoelectric complex, the Cl^- cationic lipid counterions reduce their electrochemical potential by entering the complex. The lipid intake will be bound by the repulsion of excess cationic bilayers inside the complex, limiting the increase of d_{DNA} and positive charge of the complexes. Because the liposomes contain a mixture of neutral and positive lipids, it is possible that lipid composition (Φ_{PC}) can be different in the complex and excess liposomes. This effect should be small, because we found no demixing in DOPC/DOTAP bilayers with $\Phi_{PC} < 0.75$.

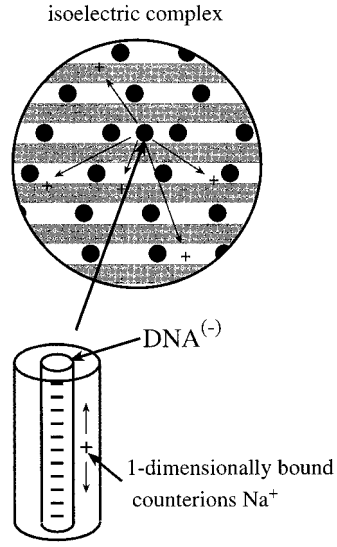

FIGURE 5 Schematic of a DNA molecule with a 1-dimensionally bound layer of condensed Na^+ counterions (~1.2 M concentration near DNA surface) and a lamellar isoelectric (charge-neutral) complex with no counterions inside it. The total free energy of this system is lowered when the excess DNA molecule enters the complex, releasing its bound counterions into the complex internal volume. Thus, the formation of negatively overcharged complexes with higher DNA packing density is driven by an osmotic concentration gradient between counterions near excess DNA and inside the isoelectric complex. An analogous mechanism due to concentration gradient between excess cationic membrane Cl^- condensed counterions and counterion-free isoelectric complex leads to the formation of positively overcharged complexes.

Recently, Bruinsma (1998) has developed an analytical solution of the Poisson–Boltzman equation for the complexes with very high Φ_{PC}, when the counterion effects dominate over the membrane and DNA electrostatic repulsion. The physical meaning of his theory corresponds to the qualitative arguments given above. We show the prediction of his calculation for the complex with $\Phi_{PC} = 0.7$ as a solid line in Fig. 4 *a*, and it is in excellent agreement with the data. However, the $d_{DNA}(\rho)$ curves change as a function of Φ_{PC} because the free energy of lipid membranes and the electrostatic repulsion of DNA and bilayers depend on σ_c. Qualitatively, the complex unit cell (Fig. 3 *b*) in the limit of no added salt can be approximated as a box with an average excess negative charge smeared on DNA walls for $\rho < 2.2$ and positive charge on lipid surfaces for $\rho > 2.2$. Treating the bilayer surfaces as flat plates, we can use the following expression for the electrostatic free energy/unit cell of positively charged ($\rho > 2.2$) complex (Lekkerkerker, 1989),

$$F_c^+ = d_{DNA}\left[\frac{4k_BT\sigma^+}{e}\left(\ln\left(\frac{2l_D}{l_C}\right) - 1\right) + \frac{\pi k_BT}{l_B\delta_w}\right]. \quad (5)$$

The first term in Eq. 5 is the free energy of a bilayer surface with excess cationic density $\sigma^+ = \sigma_c(1 - d_{DNA}^{iso}/d_{DNA})$ and the second is the repulsive free energy (Langmuir pressure) of two bilayers separated by a distance $\delta_w \gg l_C$ (Israelachvili, 1992). The Chapman length, $l_C = e/(2\pi\sigma^+ l_B)$, corresponds to the thickness of condensed counterion layer near

the membrane surface and $l_D \gg l_C$ (no salt) is the Debye screening length. The Bjerrum length $l_B = e^2/\epsilon k_B T \approx 7.1$ Å in water ($\epsilon = 78.5$) at room temperature. F_c^+ should be compared with the free energy F_B of excess cationic membrane of length d_{DNA},

$$F_B = d_{DNA}\left[\frac{4k_BT\sigma_c}{e}\left(\ln\left(\frac{2l_D}{l_C}\right) - 1\right)\right]. \quad (6)$$

Because $\sigma_c > \sigma^+$ so that $F_c^+ < F_B$, the complex will take in all the available excess membrane until stopped by the second repulsive term in the Eq. 5. This also implies greater affinity for excess lipid in complexes with larger σ_C. Thus, d_{DNA} increase over a larger range of ρ values in complexes with lower Φ_{PC}, consistent with the data of Fig. 4 *a*.

In complexes with $\rho < 2.2$, electrostatic energy of anionic complex,

$$F_c^- = \delta_w\left[\frac{4k_BT\sigma^-}{e}\left(\ln\left(\frac{2l_D}{l_C}\right) - 1\right) + \frac{\pi k_BT}{l_B d_{DNA}}\right], \quad (7)$$

should be compared with the free energy of charged DNA rods in solution. Equation 7 oversimplifies the complex unit cell structure by treating DNA surfaces as being flat. This, however, does not change the fact that because the complex excess anionic charge density $\sigma^- = \sigma_{DNA}(1 - d_{DNA}/d_{DNA}^{iso})$ is smaller than the charge density σ_{DNA} of free DNA, the latter will enter the complex until stopped by the growth of σ^- and the repulsive energy of DNA strands. Because DNA repulsion is weaker in complexes with larger d_{DNA}^{iso} (larger Φ_{PC}), they will absorb more DNA and acquire greater anionic charge, consistent with the data of Figs. 3 *b* and 4 *a*. Thus, the overall shift of the $d_{DNA}(\rho)$ curves for different Φ_{PC} is primarily due to the relative magnitudes of inter-DNA and bilayer electrostatic repulsion. A recent numerical solution of lamellar CL-DNA complex structure based on the principles similar to our above discussion have captured correctly this qualitative feature of the data (Harries et al., 1998).

A sensitive measurement of the affinity of the complexes with different Φ_{PC} for excess DNA and lipid is provided by the analyses of $d_{DNA}(\Phi_{PC})$ variation in complexes with different ρ (Fig. 4 *c* and *d*). The raw data of Fig. 4 *c* is plotted as a function of $\rho/(1 - \Phi_{PC})$ to facilitate comparison with the Eq. 4, which is shown as a solid line. This expression is consistent with the behavior of d_{DNA} in isoelectric ($\rho = \rho^{iso} = 2.2$) complexes. Therefore, if complexes with $\rho \neq 2.2$ would expel all excess lipid or DNA, the d_{DNA} curves would differ only by a multiplicative factor in complexes with different ρ. The data, scaled to $\rho_{iso} = 2.2$ (i.e., multiplied by ρ_{iso}/ρ), is shown in Fig. 4 *d*. The d_{DNA} curves do not overlap, but rather systematically deviate from the reduced ρ_{iso} prediction given again by the solid line. The data points lying above the ρ_{iso} line correspond to the complexes that have taken in excess lipid, with larger deviation for complexes with greater lipid affinity. Similarly, the points below the line have excess DNA. The complex affinity for excess cationic lipid is inversely proportional to Φ_{PC}, while its affinity for excess anionic DNA increases with Φ_{PC}. This is in excellent agreement with the counterion osmotic pressure model of complex overcharging presented above and the $d_{DNA}(\rho)$ data of Fig. 4 *a*.

The counterion-based interactions, which determine the structure of complexes with different Φ_{PC} away from the isoelectric point, should be sensitive to the solution ionic strength. The salt co-ions will act to compensate the difference in counterion concentration within the complex and excess liposomes or DNA. The counterion osmotic pressure driving excess cationic lipid into the complex will disappear when the concentration of identical salt ion species becomes equal to the concentration of counterions near the excess lipid bilayers. Because most of these counterions are confined within a layer of thickness l_c (Chapman layer), this condition can be written as

$$c^- = \sigma_c/l_C = (1 - \Phi_{PC})^2(2\pi l_B)/(a^2 e) = c^*[\text{NaCl}]. \quad (8)$$

Therefore, a given salt concentration will only affect complexes with higher Φ_{PC}, without much effect on the complexes of higher lipid charge density. We show in Fig. 4 *b* the $d_{DNA}(\rho)$ curves in the presence of 150 mM NaCl for complexes with $\Phi_{PC} = 0$, 0.5, and 0.7. In the complexes with $\Phi_{PC} = 0.7$, d_{DNA} undergoes only a small increase near the isoelectric point, so that little excess DNA or lipid enters the complex. Therefore, these complexes remain nearly charge-neutral. For the two lower Φ_{PC} the effect of added salt is smaller. This is because $c^* \sim 100$ mM for $\Phi_{PC} = 0.7$, whereas $c^* \sim 280$ mM and 1 M in complexes with $\Phi_{PC} = 0.5$ and 0. Note that the Debye length $l_D \sim 8$ Å is smaller then the distance between the surfaces of DNA molecules ($d_{DNA} - 20$ Å) for most of the data in Fig. 4 *b*, so that a simple Coulomb screening cannot account for the observed salt effect. This finding is particularly important for transfection applications of CL-DNA complexes, because the elevated ionic strength in cell culture solutions and in tissues will act to modify the complex overcharging. The low excess charge of high Φ_{PC} complexes at 150 mM may make them less efficient as transfection agents.

We further investigate the dependence of complex structure on the ionic strength in Fig. 6, where we show the dependence of d and d_{DNA} on NaCl concentration M in isoelectric complexes with different Φ_{PC}. The $d_{DNA}(M)$ dependence is nonmonotonic in samples with $\Phi_{PC} \geq 0.5$ (Fig. 6 *a* and *c*), slightly increasing for low M and decreasing steeply at higher M. The crossover between the two regimes occurs at $M \sim 90$ mM for $\Phi_{PC} = 0.7$ and 170 mM for $\Phi_{PC} = 0.6$, very close to $c^* = 100$ mM and 180 mM given by Eq. 8. For $M > c^*$ we observe increase of the multilayer repeat distance d and expulsion of excess lipid from the complexes (seen both in x-ray diffraction and fluorescence). The salt screens the counterion-release mechanism, resulting in gradual release of cationic lipid from the complex with increasing M and effective shift of the complex equilibrium structure toward the negative ($\rho < 2.2$) side of the phase diagram. This shift, accompanied by a

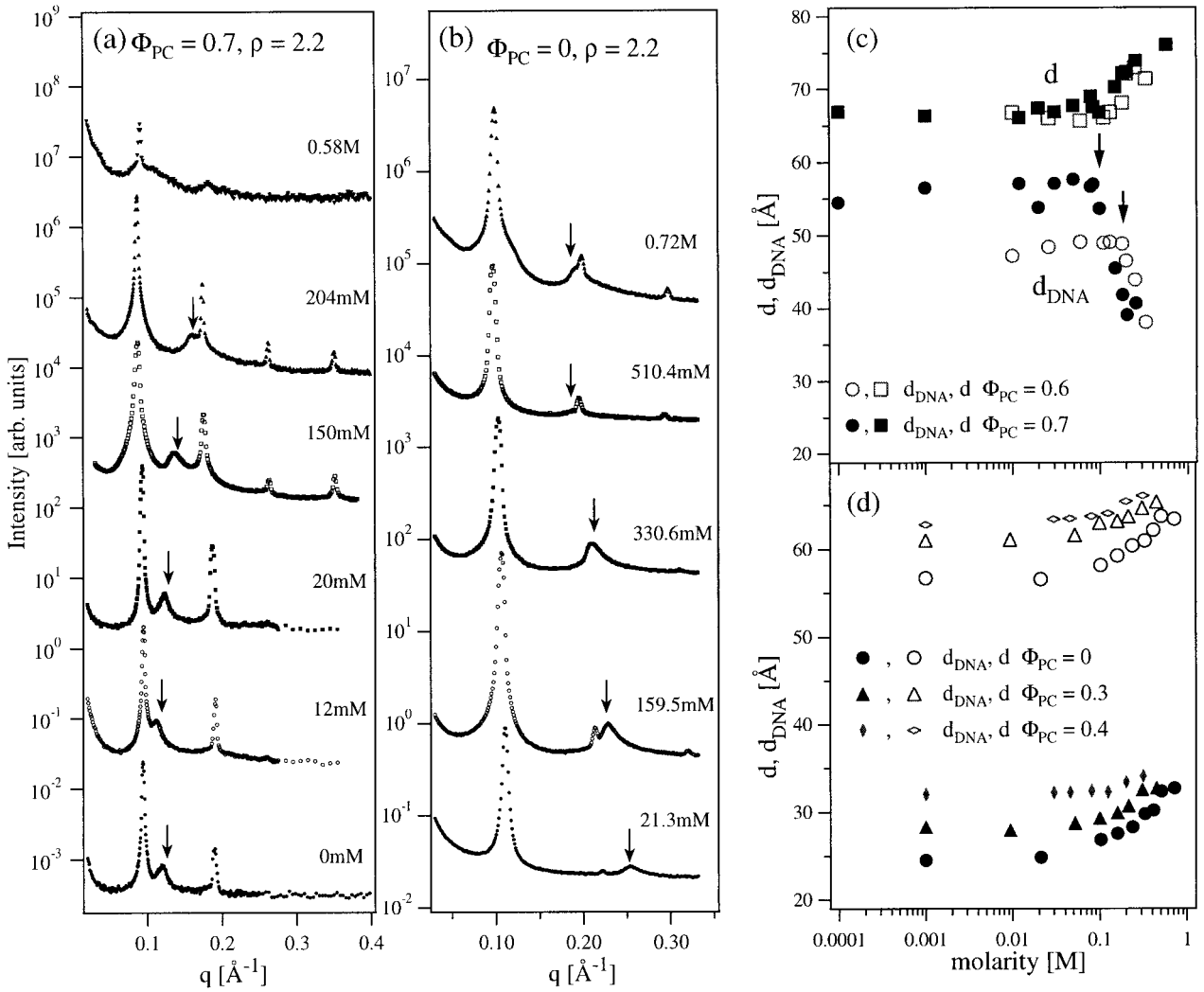

FIGURE 6 (*a*) and (*b*) Synchrotron SAXS scans of isoelectric complexes with $\Phi_{PC} = 0.7$ (*a*) and $\Phi_{PC} = 0$ (*b*) as a function of the increasing solution ionic strength, controlled by the addition of NaCl. Arrows indicate the position of DNA correlation peaks. (*c*) and (*d*) Variation of the isoelectric complex structure as a function of the monovalent salt NaCl concentration for high $\Phi_{PC} > 0.5$ (*c*) and for low $\Phi_{PC} < 0.5$ (*d*). Arrows in (*c*) indicate the concentration c^* given by the Eq. 8.

decrease of d_{DNA} down to ~38 Å is favored in complexes with $\Phi_{PC} > 0.5$, as seen in Fig. 4 *a*. The accompanying increase in d is due to the expansion of the DNA–water layer thickness between the membranes and is another consequence of the weakening cohesion of the complex. This can also be seen from the SAXS scans of Fig. 6 *a*, where the data at $M > c^*$ shows broadening of the lamellar peak because of an increasing disorder in weakened CL-DNA stacks. The increase of d may also partially result from the screening of cationic lipid headgroup charge. This reduces the lipid headgroup area and increases the bilayer thickness δ_m, but no more than by ~3 Å. The complex completely dissociates at even higher salt concentrations (*top scan* at 0.58 M in Fig. 6 *a*).

The slight increase of d_{DNA} at constant d for $M < c^*$ with increasing M (Fig. 6 *c*) implies a slight reduction of the DNA quantity in the complex. It is harder to explain qualitatively, considering that the concentrations of counterions near the charged DNA and lipid surfaces, which ultimately determine d_{DNA}, are only weakly sensitive to the low bulk co-ion concentrations (Le Bret and Zimm, 1984; Sharp, 1995). It would be valuable to have a complete quantitative explanation of the $d_{DNA}(M)$ dependence, which requires a numerical solution of the nonlinear Poisson–Boltzman equation in the presence of salt.

The variation of complex structure with M is completely different for high membrane charge density $\Phi_{PC} \leq 0.4$, were d_{DNA} increases monotonically with M at salt concentrations smaller then c^* (Fig. 6 *b* and *d*). The salt concentration in this regime also remains smaller than the concentration of condensed counterions around the DNA double strands (~1.2 M) (Manning, 1978). This increase in d_{DNA} is accompanied by a release of DNA from the complexes into solution. The large monotonic increase of d_{DNA} with M for $\Phi_{PC} \leq 0.4$ at salt concentrations lower than c^* suggests the presence of an additional nonelectrostatic repulsion between

DNA strands, which pushes DNA out of complexes as electrostatic interactions (which define $d_{DNA} = d^{iso}_{DNA}$ as given by Eq. 4) are gradually screened by the added salt. We propose that this additional interaction is the hydration repulsion between the DNA strands (Rau et al., 1984). Exponentially decaying hydration forces are insensitive to monovalent salt concentrations and have been shown to dominate the interstrand repulsion in bulk DNA phases up to the distances of ~32–35 Å (Podgornik et al., 1994). Thus, they would contribute little to the interactions in complexes with high Φ_{PC}. This is in excellent agreement with the data of Fig. 6, where only samples with $d^{iso}_{DNA} < 32$ Å exhibit the monotonic increase of d_{DNA} with M, approaching 35 Å at high M independent of Φ_{PC}. Our recent measurement of the compressional modulus of DNA lattice in isoelectric complexes using the x-ray line-shape analyses of DNA correlation peak have also indicated the presence of repulsive hydration force in samples with $\Phi_{PC} < 0.4$ (Salditt et al., 1998).

DISCUSSION

Figure 7 *a* shows the phase diagram of the L^c_α CL-DNA complexes. The complexes always reverse charge at stoichiometrically neutral ratio of DNA and DOTAP ($\rho = 2.2$, *broken line*), where their structure is in agreement with a complete counterion release upon lipid-DNA binding. This creates a negative counterion osmotic pressure driving excess lipid and DNA into the complex with $\rho \neq 2.2$ and results in overcharged anionic and cationic complexes useful as nonviral gene vectors. Electrostatic repulsion sets a limit on the amount of excess DNA or lipid that can enter a complex and leads to the increasing width of the single-phase complex region with decreasing Φ_{PC}. Significantly, most of the phase diagram features are explained within a nonlinear Poisson–Boltzman electrostatic model, in spite of it completely neglecting the details of DNA and lipid molecular structure. Thus, we can expect it to be applicable to nonspecific association of many oppositely charged biological macromolecules clarifying, for example, the limited negative overcharging of nucleosomes. We emphasize that the successful explanation of the complex phase diagram depended critically on considering free energies of the whole DNA/lipid/complex system—a point that should apply to all the macromolecular assemblies within the dense cytoplasm.

Related to the phase diagram is the colloidal stability of individual ~0.2 μm complexes against aggregation and coalescence, which is a required property for their gene-delivery applications (Fig. 7 *b*). Only the one-phase complexes of lower charge aggregate, so that colloidal stability is lowest in complexes with $\Phi_{PC} = 0$, which aggregate over the broadest range of ρ. However, because the complex aggregates are very polydisperse, their size will depend strongly on total lipid and DNA concentration. The data of Fig. 7 *b* was obtained with concentrations typically used in cell-culture transfections, where the complexes with $\Phi_{PC} = 0.7$ were found to be relatively stable (concentration below a critical aggregation concentration), whereas at $\Phi_{PC} = 0$ the size of aggregates was diverging. This variation of the colloidal stability may additionally be caused by the changes in surface free energy of the spherical 0.2 μm complexes. The DNA-lipid layers of the L^c_α complex have to curve to terminate the complex surface with the hydrophilic lipid headgroups of the lipid bilayers. It is likely that the energy penalty of the associated liquid crystalline defects will be larger for complexes with smaller Φ_{PC}, because the combined bending stiffness of the DNA-lipid layers increases with the DNA packing density (Salditt et al., 1998).

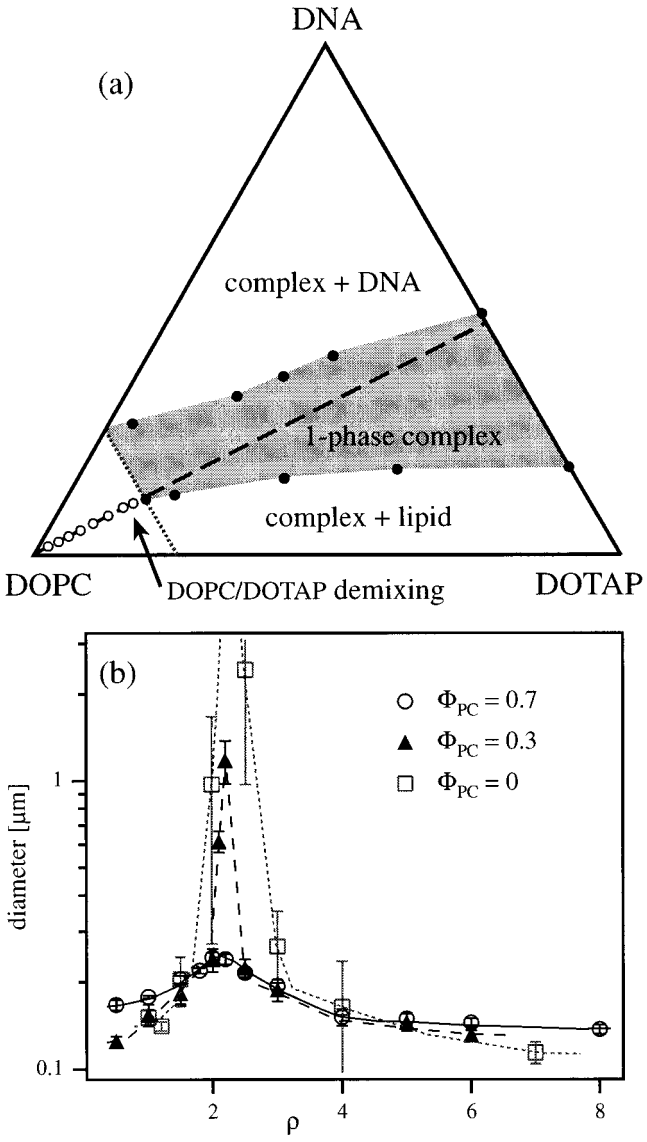

FIGURE 7 (*a*) Phase diagram of the lamellar CL-DNA complexes. Corners of the triangle correspond to 100% weight fraction of DOPC, DOTAP, and DNA. Dashed line indicates the isoelectric DOTAP/DNA ratio. (*b*) Colloidal aggregation of complexes in the different regions of the phase diagram at concentrations typically used in transfection experiments and at low (~10 mM) solution ionic strength.

Therefore, the complexes with smallest Φ_{PC} have the largest surface free energy and will aggregate to decrease the overall surface of the bulk L_α^c phase.

During a transfection experiment, the CL-DNA complexes are subjected to varying solution ionic strength in the cell culture media and in the cytosol. The phase diagram of Fig. 7 *a* is directly related to the stability of complexes at elevated ionic strength. The complexes become unstable and charge neutral at monovalent salt concentrations $M > c^* \sim (1 - \Phi_{PC})^2$ (Eq. 5), so that their stability decreases quickly with decreasing membrane charge density (increasing d_{DNA}). This should be kept in mind in designing the complexes for cell transfection, because, at $M > 100$ mM, the low Φ_{PC} complexes will interact weakly with anionic cellular membranes, but dissociate easily with increased ionic strength (e.g., inside endosomal vesicles). These effects arise because the salt co-ions at concentrations $M > c^*$ alter the osmotic pressure of ions inside the complex and near DNA and bilayer surfaces. Thus the added salt changes the very interactions driving the complex formation, rather than simply screening Coulomb repulsion of DNA and bilayers. Similar effects of ionic strength can be expected in other complexes of oppositely charged macroions. In fact, because many proteins can be altered by post-translational modification, we can imagine that alteration of a protein surface charge density can serve as a control mechanism of nonspecific protein-DNA association at physiological salt concentrations.

Comparison of the different added salt effects on DNA packing in high and low Φ_{PC} complexes also reveals the additional nonelectrostatic repulsive hydration force between the DNA molecules at separations below ~35 Å. The presence of this force can also be seen affecting the curvature of 1 − phase complex/complex + DNA coexistence line below $\Phi_{PC} \sim 0.4$ of the phase diagram (Fig. 7 *a*). The range of hydration force identified here is similar to that observed in bulk DNA phases, indicating that it is not affected by the DNA confinement between the lipid membranes. This force should be considered in the evaluation of other condensed DNA structures.

We thank J. N. Israelachvili, P. Pincus, N. Dan, G. C. L. Wong, J. O. Rädler, and especially R. Bruinsma for useful discussions. Supported by the University of California Biotechnology Research and Education Program Grant No. 97-02, NSF-DMR-9624091, and National Institutes of Health 1 ROIGM59288-01. T.S. acknowledges a Nato postdoctoral scholarship distributed by the DAAD. The Materials Research Laboratory at Santa Barbara is supported by NSF-DMR-9632716. The synchrotron x-ray experiments were carried out at the SSRL supported by the U.S. Department of Energy.

REFERENCES

Bruinsma, R. 1998. Electrostatics of DNA cationic lipid complexes: isoelectric instability. *Eur. Phys. J. B.* 4:75–88.

Felgner, P. L., and G. Rhodes. 1991. Gene therapeutics. *Nature.* 349: 351–352.

Felgner, P. L. 1997. Nonviral strategies for gene therapy. *Sci. Am.* 276: 102–106.

Gustafsson, J., G. Arvidson, G. Karlsson, and M. Almgren. 1995. Complexes between cationic liposomes and DNA visualized by cryo-TEM. *Biochim. Biophys. Acta.* 1235:305–312.

Harries, D., S. May, W. Gelbart, and A. Ben Shaul. 1998. Structure, stability, and thermodynamics of lamellar DNA-lipid complexes. *Biophys. J.* 75:159–173.

Harrington, J. J., G. VanBokkelen, R. W. Mays, K. Gustashaw, and H. F. Willard. 1997. Formation of de novo centromeres and construction of first-generation human artificial microchromosomes. *Nat. Genet.* 15: 345–355.

Israelachvili, J. N. 1992. Intermolecular and Surface Forces. Academic Press, San Diego, CA.

Koltover, I., T. Salditt, J. O. Rädler, and C. R. Safinya. 1998. An inverted hexagonal phase of cationic liposome-DNA complexes related to DNA release and delivery. *Science.* 281:78–81.

Lasic, D. D., H. Strey, M. C. A. Stuart, R. Podgornik, and P. M. Frederik. 1997. The structure of DNA-liposome complexes. *J. Am. Chem. Soc.* 119:832–833.

Le Bret, M., and B. H. Zimm. 1984. Distribution of counterions around a cylindrical polyelectrolyte and Manning's condensation theory. *Biopolymers.* 23:287–312.

Lekkerkerker, H. N. W. 1989. Contribution of the electric double layer to the curvature elasticity of charged amphiphilic monolayers. *Physica A.* 159:319–328.

Manning, G. S. 1969. Limiting laws and counterion condensation in polyelectrolyte solutions. I. Colligative properties. *J. Chem. Phys.* 51: 924–933.

Manning, G. S. 1978. The molecular theory of polyelectrolyte solutions with applications to the electrostatic properties of polynucleotydes. *Quart. Rev. Biophys.* 2:179–246.

Mascotti, D., and T. M. Lohman. 1990. Thermodynamic extent of counterion release upon binding oligolysines to single-stranded nucleic acids. *Proc. Natl. Acad. Sci. USA.* 87:3142–3146.

Misra, V., K. Sharp, R. Friedman, and B. Honig. 1994. Salt effects on ligand-DNA binding: minor groove binding antibiotics. *J. Mol. Biol.* 238:245–263.

Nabel, G. J., E. G. Nabel, Z. Y. Yang, B. A. Fox, G. E. Plautz, X. Gao, L. Huang, S. Shu, D. Gordon, and A. E. Chang. 1993. Direct gene transfer with DNA liposome complexes in melanoma-expression, biologic activity and lack of toxicity in humans. *Proc. Natl. Acad. Sci. USA.* 90:11307–11311.

Podgornik, R., D. C. Rau, and V. A. Parsegian. 1994. Parametrization of direct and soft steric-undulatory forces between DNA double helical polyelectrolytes in solutions of several different anions and cations. *Biophys. J.* 66:962–971.

Rädler, J. O., I. Koltover, T. Salditt, and C. R. Safinya. 1997. Structure of DNA-cationic liposome complexes: DNA intercalation in multilamellar membranes in distinct interhelical packing regimes. *Science.* 275: 810–814.

Ramakrishnan, V. 1997. Histone structure and the organization of the nucleosome. *Annu. Rev. Biophys. Biomol. Struct.* 26:83–112.

Rau, D. C., B. Lee, and V. A. Parsegian. 1984. Measurement of the repulsive force between polyelectrolyte molecules in ionic solution: hydration forces between parallel DNA double helices. *Proc. Natl. Acad. Sci. USA.* 81:2621–2625.

Salditt, T., I. Koltover, J. O. Rädler, and C. R. Safinya. 1997. Two-dimensional smectic ordering of linear DNA chains in self-assembled DNA-cationic liposome mixtures. *Phys. Rev. Lett.* 79:2582–2585.

Salditt, T., I. Koltover, J. O. Rädler, and C. R. Safinya. 1998. Self-assembled DNA-cationic-lipid complexes: two-dimensional smectic ordering, correlations, and interactions. *Phys. Rev. E.* 58:889–904.

Schlax, P. J., M. W. Capp, and M. T. Record. 1995. Inhibition of transcription initiation by lac repressor. *J. Mol. Biol.* 245:331–350.

Sharp, K. A. 1995. Polyelectrolyte electrostatics—salt dependence, entropic, and enthalpic contributions to free energy in the nonlinear Poisson–Boltzmann model. *Biopolymers.* 36:227–243.

Zhu, N., D. Liggitt, Y. Liu, and R. Debs. 1993. Systematic gene expression after intravenous DNA delivery into adult mice. *Science.* 261:209–211.